PNAS
www.pnas.org

Supplementary Information for

Aryl hydrocarbon receptor is essential for the pathogenesis of pulmonary arterial hypertension

Takeshi Masaki[1], Makoto Okazawa[1], Ryotaro Asano, Tadakatsu Inagaki,

Tomohiko Ishibashi, Akiko Yamagishi, Saori Umeki-Mizushima, Manami Nishimura,

Yusuke Manabe, Hatsue Ishibashi-Ueda, Manabu Shirai, Hirotsugu Tsuchimochi,

James T. Pearson, Atsushi Kumanogoh, Yasushi Sakata, Takeshi Ogo,

Tadamitsu Kishimoto*, Yoshikazu Nakaoka*

[1]T.M. and M.O. contributed equally to this work.

* Tadamitsu Kishimoto and Yoshikazu Nakaoka
Email: kishimoto@ifrec.osaka-u.ac.jp.
Email: ynakaoka@ncvc.go.jp

This PDF file includes:

Supplementary text
Figures S1 to S5
Tables S1 to S2
SI References

Supplementary Method

Human samples

All protocols using human specimens were approved by the Institutional Review Board of the National Cerebral and Cardiovascular Center, Suita, Japan (M30-060, M30-168). Peripheral blood samples for the AHR luciferase reporter assay were obtained from PAH patients (n=18) and HV (n=16) between October 2018 and May 2019. The average ages (means ± SD) of PAH patients and HV were 47.6 ± 14.4 and 44.1 ± 10.1 years, respectively. Peripheral blood samples for RNA-seq analysis were obtained from PAH patients (n=2) and HV (n=2). Lung tissues were obtained at autopsy from patients who died of PAH (n=4) and from control patients (n=4) who died of other causes (such as cerebral bleeding). All lung specimens were obtained at the National Cerebral and Cardiovascular Center Hospital, and all patients and their bereaved families provided written consent for the use of their lung tissues for biomedical research. The average ages (means ± SD) of PAH patients and controls were 41.0 ± 2.8 and 71.3 ± 9.7 years, respectively. The resected lung tissues were immediately fixed with 10% buffered formalin, followed by embedding in paraffin for serial sectioning for immunohistochemical staining. Characteristics of patients and controls are provided in *SI Appendix,* Tables S1and S2.

Animals

All experiments were carried out under the guidelines and Animal Ethics Committee of the National Cerebral and Cardiovascular Center Research Institute and approved by the Institutional Review Board of the National Cerebral and Cardiovascular Center. Male Sprague–Dawley (SD) rats aged 6–9 weeks (150–250 g) (Charles River Laboratories) were used in the animal experiments except for *SI Appendix,* Fig. S2 *E*-*G*. For *SI Appendix,* Fig.S 2*E*-*G*, female SD rats aged 6–9 weeks (150–200 g) were used. *Ahr*$^{-/-}$ rats were created at the Experimental Animal Sciences Faculty of Medicine, Osaka University, using the CRISPR/Cas9 system. 6-week-rats were used for the analysis of the renal morphology and the measurements of serum biochemical parameters which were measured with Catalyst One (IDEXX Laboratories, Inc.). In animal experiments, littermates or animals treated with vehicle (carboxymethylcellulose, 0.5%; sodium chloride, 0.9%; polysorbate 80, 0.4%; benzyl

alcohol, 0.9% in sterilized water) were used as controls. For administration of all drugs except for FICZ (Ark Pharm), i.e., SU5416 (MedChemExpress), Ki8751 (Adooq Bioscience), TAK-593 and indirubin (Adooq Bioscience), rats were injected once subcutaneously at a dose of 20 mg/kg body weight, and then exposed to hypoxia (10% O_2) for 3 weeks, followed by normoxia (21% O_2) for 2, or 5 weeks. In experiments using FICZ-treated rats (FICZ/Hx/Nx or FICZ/Nx), rats were injected subcutaneously with FICZ (10 mg/kg body weight/week) every week until hemodynamic measurements were performed, with or without exposure to hypoxia (10% O_2) during the first 3 weeks. In the experiment using Qing-Dai, Qing-Dai was administered at 3 g/kg body weight/day in pulverized chow (Roden CAFÉ; Oriental Yeast) with exposure to hypoxia (10% O_2) for the first 3 weeks. The dosage of Qing-Dai was determined according to the previous report (1). Experimental groups and control groups were randomly assigned. The hemodynamic measurements were done blindly, and the data analysis was performed independently by 2 researchers.

Hemodynamic measurements

During hemodynamic measurements, rats were anesthetized with isoflurane (induction 3%, maintenance 1.0–1.5% mixed with room air), and the trachea was cannulated for mechanical ventilation. The body temperature was maintained at 37–38°C using a rectal thermistor coupled with a thermostatically controlled heating pad. The right carotid artery was isolated and cannulated with a PE-50 catheter filled with heparinized saline for systemic blood pressure measurement. An 18-gauge BD Angiocath catheter (Becton Dickinson) was inserted into the right jugular vein and advanced into the right ventricle (RV) to measure right ventricular pressure. The pressure signals were relayed to a BP Amp (ML117; AD Instruments). Data acquisition was performed using the PowerLab data system (AD Instruments). Heart rate (HR) was derived from the arterial systolic peak, and mean arterial pressure (MAP) and right ventricular systolic pressure (RVSP) were calculated online. The rats which had HR < 200 bpm, MAP <50 mmHg, and obvious anatomical anomaly were excluded.

Morphometric Analyses

After hemodynamic measurements, the heart and lungs were perfused with normal saline followed by with 4% (wt/vol) paraformaldehyde (PFA) at constant pressure to fully distend the pulmonary vessels and airway, respectively. The heart and lungs were harvested, the heart was dissected, and the RV wall was removed from the left ventricle (LV) and septum. Fulton's Index, the ratio of RV to LV + septum weight [RV/(LV+S)], was calculated to evaluate the extent of right ventricular hypertrophy. Excised lungs were fixed in 4% PFA overnight and then embedded in paraffin and cut into 4-μm-thick sections. Paraffin-embedded lung sections were subjected to hematoxylin–eosin (HE) or EVG staining. Images of pulmonary arteries were captured with a virtual slide scanner (Aperio; Leica or NanoZoomer S60; Hamamatsu Photonics). PA remodeling was assessed by the percent wall thickness and luminal occlusive neointimal lesions. The percent wall thickness was calculated as the medial wall thickness (the distance between the internal and external lamina) × 2 divided by the diameter of the vessel (the distance between external lamina) × 100. For vessels with a single elastic lamina, the distance between the elastic and endothelial basement membrane was measured. Medial wall thickness was analyzed only for sectioned vessels with an approximately circular profile. Luminal occlusive neointimal lesions were assessed and scored as: no evidence of neointimal formation (open), partial luminal occlusion (<50%, partial), or severe-luminal occlusion (≥50%, closed). Pulmonary artery occlusion rate was expressed as the percentage of each grade. We assessed the luminal occlusive neointimal lesions of vessels with outer diameter (OD) <50 μm and between 50 and 100 μm. The diameter of pulmonary arteries and the grading of luminal occlusive neointimal lesions were determined using Image Scope (Leica). The percent wall thickness and pulmonary artery occlusion rate were calculated for at least 30 small arteries and arterioles for each rat. For HE staining of rat kidney, the kidneys were perfused with normal saline followed by with 4% PFA at a constant pressure. The kidneys were harvested, fixed overnight, embedded in paraffin and cut into 4-μm-thick sections.

Immunohistochemical analyses

For immunohistochemical analyses of rat lung tissues, samples were fixed in 4% PFA/ phosphate-buffered saline (PBS) for 1 h; some were cryoprotected with PBS containing 5–20% sucrose, frozen

in OCT compound (Sakura), and cut into 10-μm-thick cryosections as described previously (13). Other rat lung tissue samples fixed in 4% PFA/PBS were embedded in paraffin. Paraffin-embedded samples of rat and human lungs were cut into 4-μm-thick sections, deparaffinized, and rehydrated. The rehydrated sections were subjected to antigen retrieval by heat induction in 10 mM sodium citrate buffer, pH 6.0. All lung sections were washed in PBS, treated with 1% hydrogen peroxide in methanol for 30 min, incubated in 2% normal horse serum (for mice first antibodies) or Block Ace (UK-B80; DS Pharma Promo) for 1 h, and incubated with primary antibodies in blocking solution overnight at 4°C. The following primary antibodies were used: anti-AHR (GTX22770, GeneTex, 1:100), anti-CYP1A1 (13241-1-AP, Proteintech, 1:200), anti-MRC1 (ab64639, Abcam, 1:800), anti–α-SMA (IS611, DAKO,), anti-CD4 (GTX76318, GeneTex, 1:50 or 25229, Cell Signaling Technology, 1:100), anti–IL-21 (NBP 1-02706, Novus Biologicals, 1:200), anti–VE-Cadherin (sc-6458, Santa Cruz Biotechnology, 1:50), and then washed in PBST. For immunohistofluorescence, the washed sections were incubated with fluorescence-conjugated (Alexa Fluor 488–conjugated or Alexa Fluor 546–conjugated, Thermo Fisher Scientific, 1:200), quenched with autofluorescence for 5 min using Vector TrueVIEW Autofluorescence Quenching Kit (SP-8400; VECTOR Lab), and imaged on a fluorescence microscope (BZX-810; Keyence). For immunohistochemistry, the sections were incubated with HRP-conjugated secondary antibodies (Cell Signaling Technology, 1:200) for 1 h at room temperature, visualized using 3,3-diaminobenzidine substrate (Sigma-Aldrich), and imaged with BZX-810 or NanoZoomer S60. Negative control sections for the immunohistochemical experiments received identical treatment except for exposure to the primary antibodies**.**

Isolation of rat lung ECs

After perfusion with autoMACS Running Buffer (0.5% BSA, 2 mM EDTA) (Miltenyi Biotec) via cannulated trachea under isoflurane anesthesia, rat lungs were dissected and enzymatically digested in DMEM (supplemented with Collagenase, Dispase, DNase I) using gentleMACS Dissociator (Miltenyi Biotec). Cell suspensions were passed through 70 μm and 30 μm meshes. Collected cells were incubated with biotin-conjugated anti–rat CD31 antibody (50-112-2507; eBioscience) for 30 min at 4°C. After that, the cells were washed and incubated with anti-biotin

microbeads (Miltenyi Biotec) for 15 min at 4°C. $CD31^+$ cells were enriched using autoMACS Pro Separator (Miltenyi Biotec)**.**

qRT-PCR analysis

After hemodynamic measurements, lower lobes of rat lungs were ligated and dissected before PFA perfusion. Total RNA from rat lung tissue was extracted using TRIzol reagent (Thermo Fisher Scientific). qRT-PCR was carried out using QuantiFAST SYBR Green RT-PCR kit (Qiagen). Fluorescence data were collected and analyzed on a LightCycler 96 (Roche). Primers used in the experiments were as follows: *Cyp1a1*: Fwd 5'-TTCAGTTCAGTCCTTCCTCACA-3', Rev 5'-GAAGGCTGGGAATCCATACA-3'; *Gapdh*: Fwd 5'-AAAGGGTCATCATCTCCGCC-3', Rev 5'-AGTGATGGCATGGACTGTGG-3'

Western blot analysis of total lung tissue

Frozen lungs were homogenized in 50 mM HEPES, 100 mM sodium fluoride, 2 mM sodium orthovanadate, 4 mM EDTA, 1% Tween-20, 0.1% SDS, and cOmplete protease inhibitor mixture (Roche) using a Polytron homogenizer (PT 10-35GT; Kinematica) as previously described.[18] The precleared lysates were then resolved by SDS-PAGE and subjected to western blot analysis with anti-AHR antibody (BML-SA210-0100; Enzo Life Sciences). Anti–β-tubulin antibody (T5201; Sigma-Aldrich) was used as the internal control. The blots were developed using HRP-coupled secondary antibodies and the ECL system.

Assessment of the effect of VEGFR2 inhibition

The human microvascular endothelial cells (HMVEC) were purchased from Lonza (Switzerland). The cells were preincubated 1.5 h at 37°C with 5% CO_2, in Endothelial Cell Growth Basal Medium-2 (EBM-2, Lonza, Switzerland) containing 0.1% bovine serum albumin (BSA) with or without 100 nM SU5416, Ki8751, TAK-593, FICZ and indirubin. After stimulation with 30 nM hVEGF (V7259, Sigma-Aldrich) for 10 min, the cells were washed twice with cold HEPES buffered saline, then lysed in RIPA buffer (50 mM Tris pH7.4, 150 mM sodium chloride, 1% NP40, 0.5% sodium deoxycholate,

0.1% SDS, 1 mM EDTA cOmplete, and PhosStop phosphatase inhibitors (Roche)). The lysates then were resolved by SDS-PAGE and subjected to western blot analysis using standard procedure. Western blot analysis was performed first with anti-Phospho-VEGFR2 antibody (Tyr1175) (#2478, Cell Signaling Technology), then was stripped, reprobed with anti-VEGFR2 antibody (#2479, Cell Signaling Technology). The blots were developed using HRP-coupled second antibodies and the ECL system.

Bone marrow transplantation (BMT)

Bone marrow (BM) cells were harvested by flushing the tibias and femurs of *Ahr*$^{+/+}$ and *Ahr*$^{-/-}$ rats with PBS. The plug of whole bone marrow cells was dispersed by passage through a pipette, filtering through a 70-µm mesh, and resuspended in normal saline. Recipient *Ahr*$^{+/+}$ or *Ahr*$^{-/-}$ rats were irradiated lethally (11 Gy), and BM cells (5.0×10^6) were injected through the tail vein. Recipient rats received drinking water supplemented with antibiotics (Baytril 170 mg/ml, Bayer). Three weeks after BMT, we prepared the SuHx rat model as described above. Chimerism was 70.9 ± 13.0%, as determined by genomic qPCR of PBMCs. Rats were excluded from studies if bone marrow reconstitution failed (Chimerism <50% by genomic qPCR of PBMC).

RNA-seq analysis

Cells and tissues were lysed in TRIzol reagent, and RNA was extracted using the PureLink RNA Mini Kit (Thermo Fisher Scientific) with PureLink DNase (Thermo Fisher Scientific). RNA and library preparation integrity were verified with TapeStation (Agilent). For RNA-seq experiments on rat lungs or lung ECs, 100 ng total RNA was used as input for ribosomal depletion, followed by library preparation using TruSeq Stranded mRNA Sample Preparation Kit (Illumina). For RNA-seq experiments of rat and human PBMCs, 100 pg total RNA was used for library preparation with SMART-seq v4 Ultra Low Input RNA Kit (Takara Clontech). Sequencing was performed on the NextSeq500 instrument (Illumina). A minimum of 25 M reads per library with 75-bp paired-ends reads were generated per sample. Quality control of the resulting sequence data was performed using FastQC. Trimmed and filtered reads were aligned to the rn6 or the hg38 reference genome

using Hisat2. Genes differentially expressed in ECs or total lung tissues were defined as those with a fold change of >2.0 or >1.5, respectively, and false discovery rate (FDR) <0.05. Genes differentially expressed in human or rat PBMCs were defined as those with a fold change of >1.5 or >2.0, respectively, and $P<0.05$.

AHR luciferase reporter assay

AHR luciferase reporter assays were performed using the Human AhR Reporter Assay System (Indigo Biosciences). Human serum samples were added to the assay medium at a concentration of 10%. PAH patients were stratified into low and high AHR activity groups (n=10 and 8, respectively), using mean AHR-Luc activity as the cut-off value. Major clinical events were defined as death, lung transplantation, and hospitalization due to right heart failure. Kaplan–Meier plot analysis of event-free survival between two groups was performed using Graph Pad Prism7.

ChIP-Seq analysis

ChIP-Seq was conducted using pooled lung samples from SuHx rats at day 4, SuHx rats at 8 weeks, or normoxia control rats (day 0); three animals were used per group. Chromatin was prepared and followed by ChIP-Seq analysis with Active Motif using anti-AHR antibody (BML-SA210-0100, Enzo Life Sciences). The 75-nt sequence reads generated by Illumina sequencing (NextSeq 500) were mapped to the genome using the BWA algorithm with default settings.

Statistical analysis

All data are expressed as the means ± SD. Statistical analyses were performed using Graph Pad Prism 7 software. Comparisons of means between two groups were performed by unpaired Student's *t*-test. Differences among multiple groups were compared by one-way ANOVA with post hoc Tukey–Kramer test. $P<0.05$ was considered statistically significant.

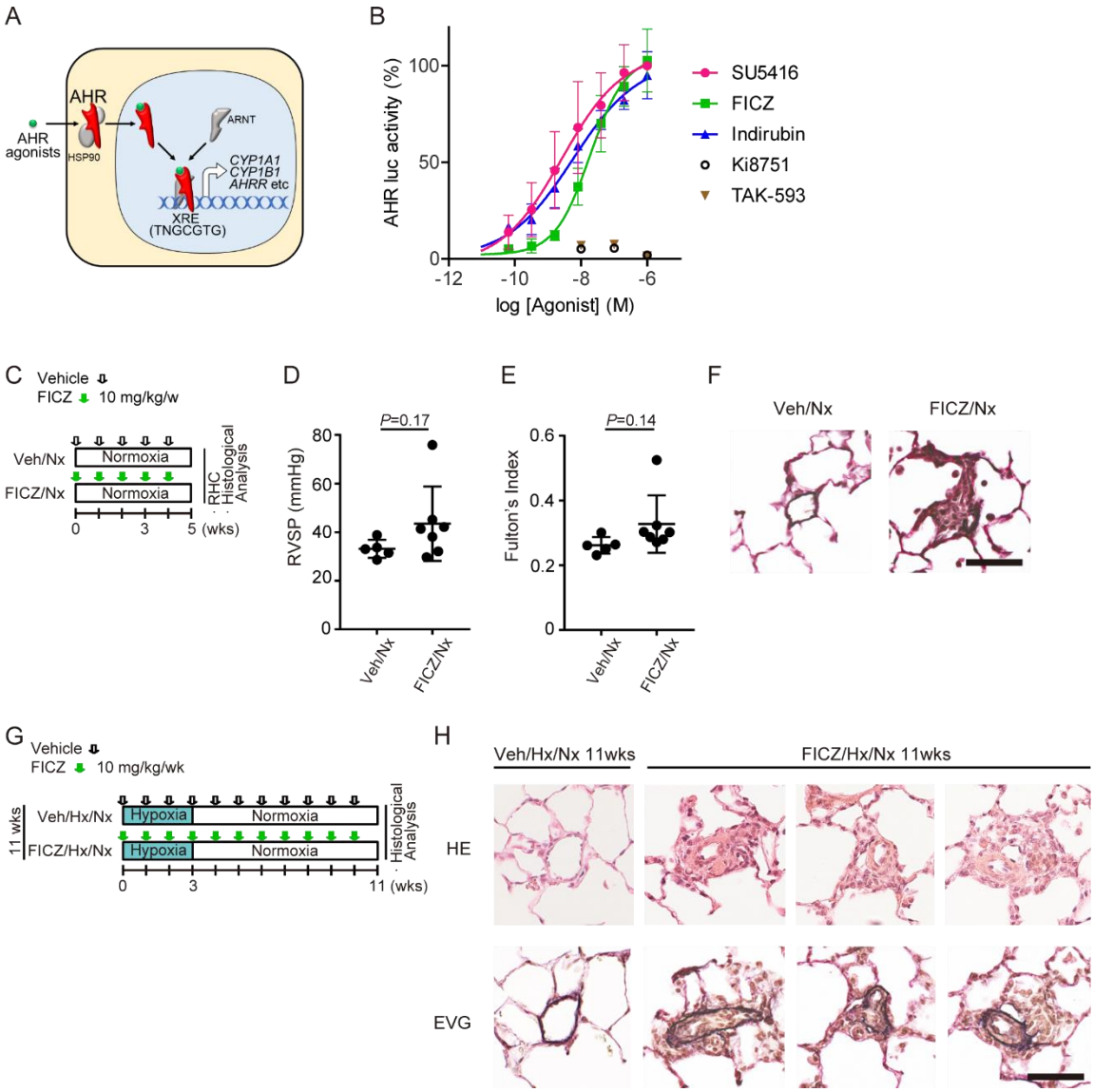

Fig. S1. AHR-Luc activity, assessed by AHR luciferase reporter assay and induction of pulmonary hypertension by the endogenous AHR agonist FICZ.

(*A*) Illustrative schema of AHR activation. AHR is localized in the cytoplasm by forming a complex with heat shock protein 90 (HSP90) and others in the absence of AHR agonists. Upon binding of AHR agonist, AHR translocates to the nucleus and forms a heterodimer with the AHR nuclear translocator (ARNT), which binds to its specific DNA sequences of the putative xenobiotic response elements (XRE) to activate transcription. (*B*) AHR-Luc activities of the chemicals used in the *in vivo* experiments in this study were evaluated by AHR luciferase assay. Data were normalized to the

maximum response to SU5416 (1 μM). (*C*) Experimental protocol for examining the effect of FICZ treatment in rats under normoxia. (*D* and *E*) Assessment of FICZ/Nx 5 wks rats (Veh: n=5; FICZ: n=7). RVSP (*D*), Fulton's index (*E*). (*F*) Representative images of vascular remodeling of distal acinar arterioles in lung sections of FICZ/Nx 5 wks rats subjected to EVG staining. Scale bar, 30 μm. (*G*) Experimental protocol for histological analysis of FICZ/Hx/Nx 11 wks rats. (*H*) Representative images of vascular remodeling of distal acinar arterioles in lung sections subjected to hematoxylin–eosin (HE) staining (upper panels) and EVG staining (lower panels) in Veh/Hx/Nx and FICZ/Hx/Nx 11 wks rats. Scale bar, 30 μm. Values are means ± SD.

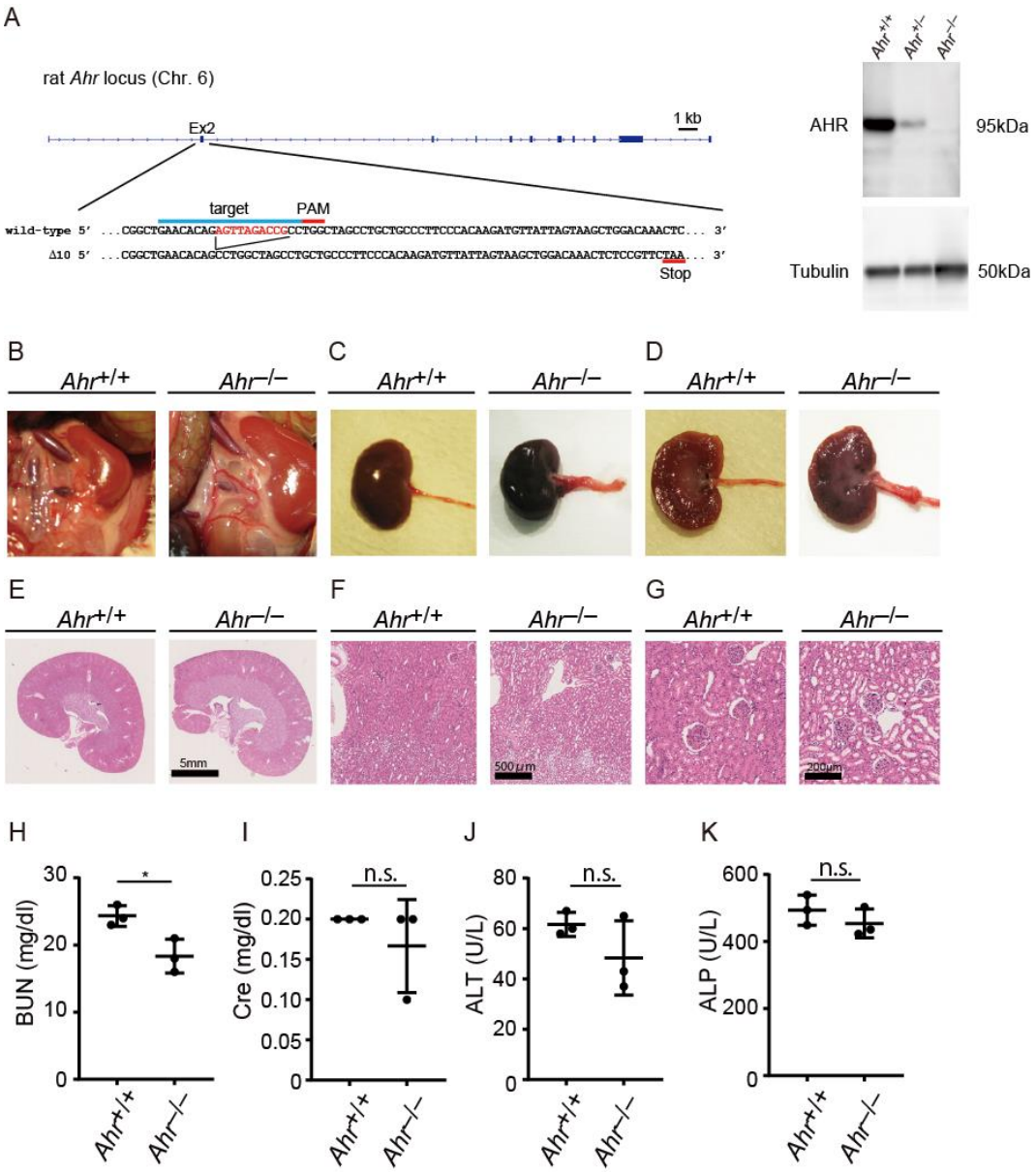

Fig. S2. The *Ahr*$^{-/-}$ rats created by CRISPR/Cas9 gene editing show almost normal function of both liver and kidney assessed by serum biochemical test.

(*A*) Generation of *Ahr*$^{-/-}$ rats: The *Ahr* gene is located on chromosome 6. *Ahr*$^{-/-}$ rats were created using CRISPR/Cas9 gene editing to delete a portion of exon 2 of *Ahr*. We confirmed knockout of AHR by western blot analysis of the lungs. Representative gross appearance of the ureters in *Ahr*$^{+/+}$ (left panel) or *Ahr*$^{-/-}$ (right panel) rats. In *Ahr*$^{+/+}$ rats, the ureters are thin and barely visible within the abdominal cavity. In *Ahr*$^{-/-}$ rats, the ureters are enlarged and tortuous. (*C*) Representative gross

images of the kidney of *Ahr*$^{+/+}$ (left panel) or *Ahr*$^{-/-}$ (right panel) rats. (*D*) Representative image of longitudinal cut of the kidney of *Ahr*$^{+/+}$ (left panel) or *Ahr*$^{-/-}$ (right panel) rats. *Ahr*$^{-/-}$ kidneys were fluid-filled and had dilated renal pelvises. Ureter at the renal hilus are enlarged in *Ahr*$^{-/-}$ rats. (*E*-*G*) HE-stained longitudinal sections of kidneys of *Ahr*$^{+/+}$ (left panel) or *Ahr*$^{-/-}$ (right panel) rats. (*H*-*K*) Serum biochemical tests of *Ahr*$^{+/+}$ and *Ahr*$^{-/-}$ rats. (*H*) Serum Blood urea nitrogen (BUN). (*I*) Serum Creatinine (Cre) (*J*) Serum alanine transaminase (ALT). (*K*) Serum alkaline phosphatase (ALP) level of *Ahr*$^{+/+}$and *Ahr*$^{-/-}$ rats. Values are means ± SD. **P*<0.05

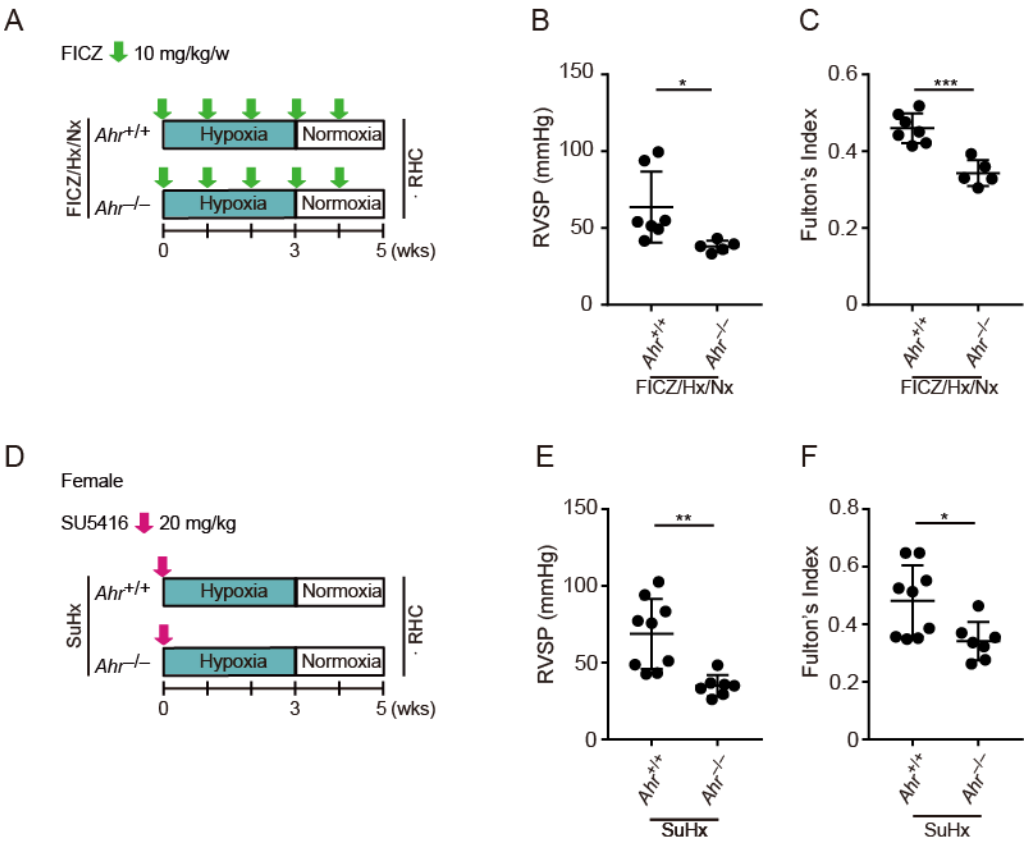

Fig. S3. *Ahr*$^{–/–}$ rats are resistant to FICZ-induced PH, and female *Ahr*$^{–/–}$ rats are resistant to SuHx.

(*A*) Experimental protocol for examining the effect of *Ahr* deletion on FICZ/Hx/Nx rats. (*B* and *C*) Assessment of the effect of *Ahr* deletion on the PH phenotype of FICZ/Hx/Nx rats (FICZ/Hx/Nx *Ahr*$^{+/+}$: n=7; FICZ/Hx/Nx *Ahr*$^{–/–}$: n=5). RVSP (*B*), Fulton's index (*C*). (*D*) Experimental protocol for examining the effect of *Ahr* deletion on female SuHx rats. (*E* and *F*) Assessment of the effect of *Ahr* deletion on the PH phenotype of female SuHx rats (SuHx *Ahr*$^{+/+}$: n=9; SuHx *Ahr*$^{–/–}$: n=7). RVSP (*F*), Fulton's index (*G*). Values are means ± SD. ***P<0.001, **P<0.01, *P<0.05

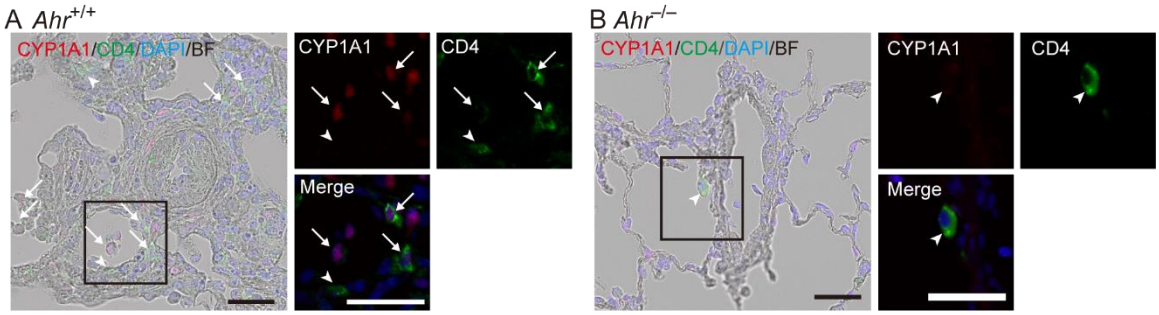

Fig. S4. CYP1A1 and CD4 Immunohistofluorescent images of pulmonary arteries of SuHx 8 wks rats.

(*A*) Representative immunohistofluorescent images of pulmonary arterioles of SuHx 8 wks *Ahr*$^{+/+}$ rats stained for CYP1A1 and CD4. Arrows indicate cells double-positive for CYP1A1 and CD4. Arrowheads indicate CD4^{+} cells that did not express CYP1A1. Scale bar, 30 μm. BF: bright field. (*B*) Representative immunohistofluorescent images of pulmonary arteries of SuHx 8 wks *Ahr*$^{–/–}$ rats stained for CYP1A1 and CD4. Arrowheads indicate CD4^{+} cells without CYP1A1 expression.

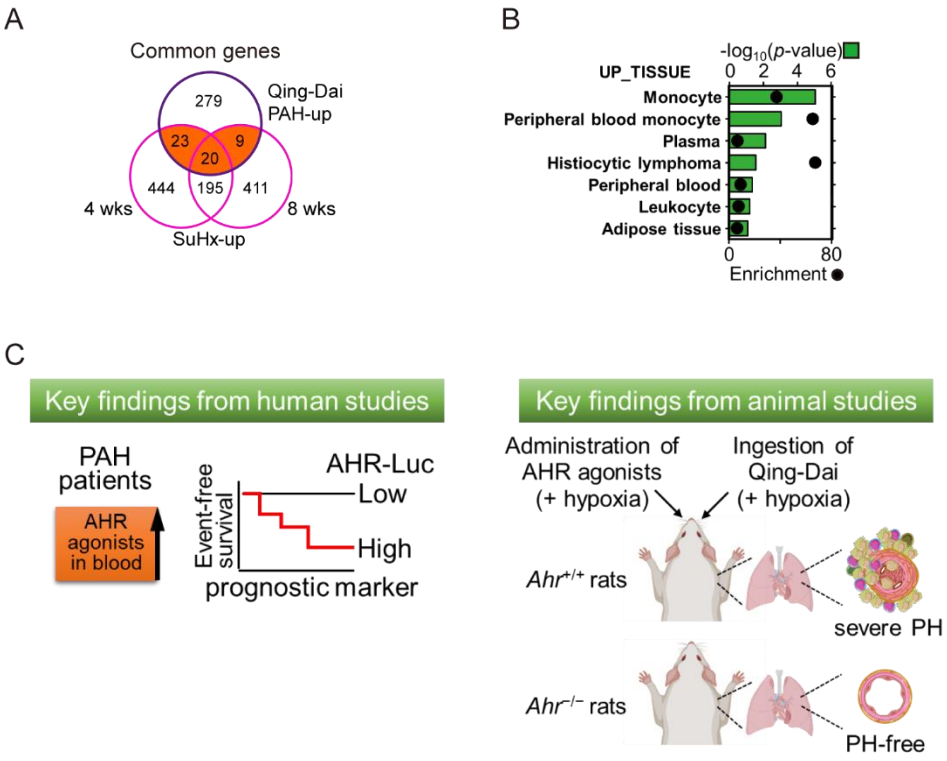

Fig. S5. Monocyte-related genes are upregulated in PBMCs of Qing-Dai–induced PAH patients and SuHx rats and key findings of this study.

(*A*) Venn diagram of genes upregulated in PBMCs of Qing-Dai–induced PAH patients and SuHx rats. Orange indicates the 52 common genes. (*B*) UP_tissue enrichment analysis of the common 52 genes. (*C*) Schematic illustration of key findings of this study.

Table S1. Characteristics of PAH patients for blood sample analyses

PAH Patients (for Luc assay)

Age (year)	Sex	Clinical diagnosis	WHO Functional Class	mPAP (mmHg)	CI (l/min/m^2)	PVR (WU)	BNP (ng/l)	6-MWD (m)
66	f	IPAH	2	23	3.98	2.5	54.1	250
43	f	HPAH	2	36	2.51	7	110.5	NA
24	f	CTD-PH	3	32	2.30	6.9	26.3	440
62	f	PoPH	2	26	2.68	5.1	31.2	440
66	f	CTD-PH	4	45	3.20	8.7	103.8	NA
48	f	HPAH	1	42	2.50	10.3	14.7	560
59	m	IPAH	3	49	2.53	6.5	74.6	380
55	m	IPAH	3	42	2.10	7.3	59.8	570
56	f	IPAH	4	82	1.37	21.9	426.3	NA
29	f	CTD-PH	3	42	2.29	12.6	40.1	525
55	f	IPAH	3	47	1.82	11.6	94.2	220
36	f	HPAH	2	68	1.97	19.2	44.3	555
59	m	PoPH	2	26	2.74	3.1	23.4	520
36	f	IPAH	2	19	3.70	2.9	9.5	450
33	f	CTD-PH	2	40	4.45	5.3	42.1	NA
41	f	IPAH	2	31	3.43	4.3	208.9	487
63	f	CTD-PH	3	29	2.51	6.6	30.7	205
25	f	IPAH	2	41	3.02	7.5	11.6	550

PAH Patients (for RNA-seq)

Age (year)	Sex	Clinical diagnosis	WHO Functional Class	mPAP (mmHg)	CI (l/min/m^2)	PVR (WU)	BNP (ng/l)	6-MWD (m)
49	m	Qing-dai - induced PH	3	44	3.49	5.2	9	510
62	f	Qing-dai - induced PH (quit)	1	11	2.72	1.5	21.4	550

Table S1. The characteristics of PAH patients are shown as above. The average age (mean ±SD) of PAH patients (n=18) and healthy volunteers (n=16) for Luc assay were 47.6±14.3 and 44.1±10.1 years, respectively. The percentages of male/female were 16.7/83.3% and 25/75%, respectively. The average age of PAH patients (n=2) and healthy volunteers (n=2) for RNA-seq were 55.5 and 39 years, respectively. IPAH: Idiopathic PAH, HPAH: Heritable PAH, CTD-PH: PAH associated with Connective tissue disease, PoPH: Portopulmonary hypertension, mPAP: mean pulmonary arterial pressure, CI: cardiac Index, PVR: pulmonary vascular resistance, BNP: B-type natriuretic peptide, 6-MWD: 6-minute walk distance

Table S2. Clinical information of PAH patients and control patients for IHC

Age (year)	Sex	Cause of Death
39	f	IPAH
45	m	IPAH
41	m	IPAH
39	f	IPAH
75	m	Cerebral Bleeding
58	m	Aortic Dissection
81	f	Cerebral Infarction, Disseminated intravascular coagulation
71	m	Cerebral Bleeding

Table S2. All lung specimens were obtained at the National Cerebral and Cardiovascular Center Hospital. The average age (means ± SD) of PAH and control patients was 41.0±2.8 and 71.3±9.7 years, respectively. IPAH: Idiopathic PAH

SI References

1. H. T. Xiao *et al.*, Qing-dai powder promotes recovery of colitis by inhibiting inflammatory responses of colonic macrophages in dextran sulfate sodium-treated mice. *Chin Med* **10**, 29 (2015).